

Near-Threshold Photoproduction of $\Lambda(1520)$ from Protons and Deuterons

N. Muramatsu,^{1,2} J.Y. Chen,^{3,4} W.C. Chang,⁴ D.S. Ahn,^{1,5} J.K. Ahn,⁵ H. Akimune,⁶ Y. Asano,² S. Daté,⁷ H. Ejiri,^{1,7} H. Fujimura,^{8,9} M. Fujiwara,^{1,2} S. Fukui,¹⁰ S. Hasegawa,¹ K. Hicks,¹¹ K. Horie,¹ T. Hotta,¹ K. Imai,⁸ T. Ishikawa,⁹ T. Iwata,¹² Y. Kato,¹ H. Kawai,¹³ K. Kino,¹ H. Kohri,¹ N. Kumagai,⁷ S. Makino,¹⁴ T. Matsuda,¹⁵ T. Matsumura,¹⁶ N. Matsuoka,¹ T. Mibe,¹¹ M. Miyabe,⁸ M. Miyachi,¹⁷ T. Nakano,¹ M. Niiyama,^{8,18} M. Nomachi,¹⁹ Y. Ohashi,⁷ H. Ohkuma,⁷ T. Ooba,¹³ D.S. Oshuev,⁴ C. Rangacharyulu,²⁰ A. Sakaguchi,¹⁹ P.M. Shagin,²¹ Y. Shiino,¹³ H. Shimizu,⁹ Y. Sugaya,¹⁹ M. Sumihama,¹ Y. Toi,¹⁵ H. Toyokawa,⁷ A. Wakai,²² C.W. Wang,⁴ S.C. Wang,⁴ K. Yonehara,⁶ T. Yorita,^{1,7} M. Yoshimura,²³ M. Yosoi,^{1,8} and R.G.T. Zegers²⁴

(LEPS Collaboration)

¹Research Center for Nuclear Physics, Osaka University, Ibaraki, Osaka 567-0047, Japan

²Kansai Photon Science Institute, Japan Atomic Energy Agency, Kizu, Kyoto, 619-0215, Japan

³Department of Physics, National Sun Yat-Sen University, Kaohsiung 804, Taiwan

⁴Institute of Physics, Academia Sinica, Taipei 11529, Taiwan

⁵Department of Physics, Pusan National University, Busan 609-735, Korea

⁶Department of Physics, Konan University, Kobe, Hyogo 658-8501, Japan

⁷Japan Synchrotron Radiation Research Institute, Sayo, Hyogo 679-5143, Japan

⁸Department of Physics, Kyoto University, Kyoto 606-8502, Japan

⁹Laboratory of Nuclear Science, Tohoku University, Sendai, Miyagi 982-0826, Japan

¹⁰Department of Physics, Nagoya University, Aichi 464-8602, Japan

¹¹Department of Physics and Astronomy, Ohio University, Athens, Ohio 45701, USA

¹²Department of Physics, Yamagata University, Yamagata 990-8560, Japan

¹³Department of Physics, Chiba University, Chiba 263-8522, Japan

¹⁴Wakayama Medical University, Wakayama, 641-8509, Japan

¹⁵Department of Applied Physics, Miyazaki University, Miyazaki 889-2192, Japan

¹⁶National Defence Academy in Japan, Yokosuka, Kanagawa 239-8686, Japan

¹⁷Department of Physics, Tokyo Institute of Technology, Tokyo, 152-8551, Japan

¹⁸RIKEN, The Institute of Physical and Chemical Research, Wako, Saitama 351-0198, Japan

¹⁹Department of Physics, Osaka University, Toyonaka, Osaka 560-0043, Japan

²⁰Department of Physics and Engineering Physics, University of Saskatchewan, Saskatoon SK S7N 5E2, Canada

²¹School of Physics and Astronomy, University of Minnesota, Minneapolis, Minnesota 55455, USA

²²Akita Research Institute of Brain and Blood Vessels, Akita, 010-0874, Japan

²³Institute for Protein Research, Osaka University, Suita, Osaka, 565-0871, Japan

²⁴National Superconducting Cyclotron Laboratory, Michigan State University, East Lansing, Michigan 48824-1321, USA

(Dated: July 3, 2018)

Photoproduction of $\Lambda(1520)$ with liquid hydrogen and deuterium targets was examined at photon energies below 2.4 GeV in the SPring-8 LEPS experiment. For the first time, the differential cross sections were measured at low energies and with a deuterium target. A large asymmetry of the production cross sections from protons and neutrons was observed at backward K^{+0} angles. This suggests the importance of the contact term, which coexists with t-channel K exchange under gauge invariance. This interpretation was compatible with the differential cross sections, decay asymmetry, and photon beam asymmetry measured in the production from protons at forward K^+ angles.

PACS numbers: 13.60.Rj, 14.20.Jn, 13.30.Eg

Recently the $\Lambda(1520)$ hyperon has received a lot of attention since its mass is close to that of the claimed pentaquark Θ^+ [1] with an opposite strangeness. Because of these features, photoproduction of $\Lambda(1520)$ from protons bears a close resemblance to that of Θ^+ from neutrons. While the experimental results of $\Lambda(1520)$ photoproduction are available in the photon energy range of 2.8–4.8 GeV from the LAMP2 Collaboration [2], this reaction has not been well understood near the threshold. Some theoretical calculations of the production cross sections were performed by considering a large contribution from t-channel vector kaon (K^*) exchange based on the cross sections and decay asymmetry measured by LAMP2 [3, 4]. However, the LAMP2 results could also be described

by a model emphasizing the importance of a contact term [5], which was necessary to conserve gauge invariance along with t-channel pseudoscalar kaon (K) exchange [6]. In this framework, a strong asymmetry is distinctively predicted in the $\Lambda(1520)$ photoproduction cross sections from protons and neutrons because a dominant contribution from the contact term is absent in the production from neutrons [5, 7]. Nevertheless, the cross section with a neutron target was not available. At low energies, the contribution from the K^* exchange was suggested to be small in a chiral unitary model [8]. Indeed, no dominance of the K^* exchange was observed in the decay asymmetry measured by the CLAS Collaboration in $\Lambda(1520)$ electroproduction at total c.m. energies up to 2.65

GeV [9]. It is unclear whether energy or photon-virtuality dependences accounts for the difference of the decay asymmetries in LAMP2 and CLAS. In most of theoretical models, the cross sections at $E_\gamma \sim 2$ GeV are predicted to be larger than those measured by LAMP2, although the difference in the model predictions is not small.

In this Letter, we report the measurements of differential cross sections, decay asymmetry, and photon beam asymmetry of $\Lambda(1520)$ photoproduction from protons and deuterons at photon energies below 2.4 GeV. We detected two charged tracks in the final state of K^+K^-p from protons or K^0K^-p from neutrons using a forward spectrometer, and the $\Lambda(1520)$ production was identified by invariant and missing mass techniques. Backward and forward productions of $\Lambda(1520)$ in the c.m. system were examined by detecting a K^+K^- or K^+p pair and a K^-p pair, respectively. These three detection modes were complementary in the acceptance. Results in all the detection modes will be presented for runs with a hydrogen target, while only those in the K^-p detection mode will be shown for runs with a deuterium target.

The experiment was carried out in 2002–2003 at the SPring-8 LEPS facility using a linearly polarized photon beam produced by backward Compton scattering of Ar laser light from 8 GeV electrons. Photons in the energy range of 1.5–2.4 GeV were tagged by detecting the recoil electrons. The photon beam with an intensity of $\sim 10^6$ /sec was alternatively injected into liquid hydrogen or deuterium targets inside a 15 cm-thick cell. The direction of linear polarization was controlled vertically or horizontally by using a half-wave plate for the laser with a polarization of nearly 100%. Charged particles were detected to analyze their momenta by the LEPS forward spectrometer [10], which covered $\pm 20^\circ$ and $\pm 10^\circ$ in the horizontal and vertical directions, respectively. Time of flight from the target to a plastic scintillator wall 4 meters downstream was measured for particle identification. Details of the experimental setup can be found in Ref. [10]. The integrated number of tagged photons reached 2.8×10^{12} (4.6×10^{12}) for the hydrogen (deuterium) runs.

The charged particles were identified within 3σ or 4σ of the momentum-dependent mass resolution. A particle decaying in flight was removed by requiring good track fitting qualities. The vertex point of two tracks was required to be within the target volume and the beam size. The missing mass of K^+K^- , K^+p , or K^-p from the proton was required to be around the proton, K^- , or K^+ mass [1], respectively. Minimum photon energies of 1.90, 1.90, and 1.75 GeV were required in the analyses with K^+K^- , K^+p , and K^-p detections, respectively, due to the limitation of the acceptance for $\Lambda(1520)$ photoproduction. Background from ϕ photoproduction was removed in the K^+K^- (K^+p) detection mode by requiring the K^+K^- invariant mass (proton missing mass) to be greater than 1.030 (1.050) GeV/c^2 . In the K^-p detection mode, such a condition was not introduced because ϕ events were kinematically limited. A resonance peak of $\Lambda(1520)$ was identified by K^+ missing mass from the proton in the K^+K^- and K^+p detection modes, and by K^-p invariant mass in the K^-p

mode, as shown in Fig. 1. The reconstructed peak positions and widths are consistent with the nominal values ($M=1519.5$ MeV/c^2 and $\Gamma=15.6$ MeV/c^2) [1] convoluted with the experimental mass resolutions (σ_M), where the contributions from momentum and photon energy resolutions are 2 MeV/c^2 and 8 MeV/c^2 , respectively. Statistics in the K^+K^- mode were relatively low, so that the K^+ polar angle region examined for the measurements of cross sections and asymmetries was limited up to 60° from the incident photon direction in the c.m. system. Instead, a larger angular region up to 90° was explored in the K^+p mode. In the K^-p mode, a K^+ ($K^{+/0}$) polar angle region above 90° (120°), defined in the c.m. system of photon and target nucleon, was examined for the hydrogen (deuterium) runs. The smaller acceptance for the deuterium runs was caused by an additional requirement that the K^-p missing mass assuming a target mass of the deuteron was smaller than 1.51 GeV/c^2 . This condition was introduced to avoid possible contaminations from additional reactions including $\gamma d \rightarrow \Lambda(1520)\Theta^+$ [11]. The cross sections remained unchanged within statistical errors even by removing this condition.

In the K^+K^- and K^-p detection modes, the background level under the $\Lambda(1520)$ resonance was estimated by two independent methods. The first method was developed on the basis of Monte Carlo (MC) simulations, which produced background spectra for the two major photoproduction processes of ϕp and nonresonant $K\bar{K}p$ final states. Small contributions other than these processes and $\Lambda(1520)$ production were in-

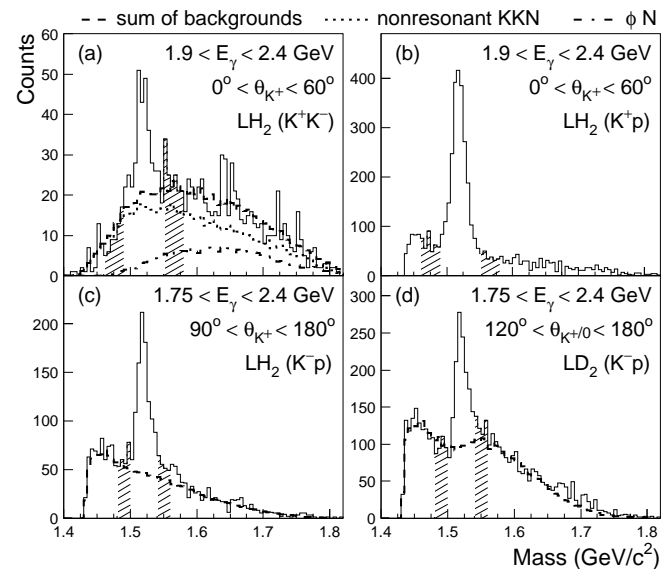


FIG. 1: Mass spectra in the four analyzed samples. Panels (a) and (b) show K^+ missing mass spectra for the hydrogen runs in the K^+K^- and K^+p detection modes, respectively. Panels (c) and (d) show K^-p invariant mass spectra in the K^-p detection mode for the hydrogen and deuterium runs, respectively. Background spectra based on Monte Carlo simulations are overlaid, while typical sideband definitions are indicated by the hatched area. The backgrounds estimated in (c) and (d) are mostly due to nonresonant $K\bar{K}p$ photoproduction.

cluded in the category of “nonresonant” process. The two background processes were generated by assuming a constant matrix element in a GEANT3-based [12] MC simulation package. In addition, the $\Lambda(1520)$ photoproduction was simulated by varying the width of the resonance depending on the phase space of decay products with the Blatt-Weisskopf barrier penetration model [13]. For the simulated events, the distributions of polar angles and momenta of the detected tracks and c.m. energy were adjusted by skimming events to reproduce the real distributions in the hydrogen runs. The skimmed MC samples were normalized so that the sum of all the samples should match the real spectra of invariant and missing masses. Quasifree photoproduction spectra from deuterons were estimated just by adopting influence of Fermi motion in the above MC samples. An off-shell correction was taken into account for a nucleon target inside deuterium. Total background spectra were expressed by summing the ϕp and nonresonant $\bar{K}\bar{K}p$ processes, as overlaid in Fig. 1. The number of $\Lambda(1520)$ signals was counted in 1.49–1.55 GeV/c^2 (1.50–1.54 GeV/c^2) over the background estimate in the K^+K^- (K^-p) mode.

In the second method, called “sideband subtraction”, the background level was estimated based on two sideband regions adjacent to the $\Lambda(1520)$ signal window, as shown by the hatched area in Fig. 1. The average of yields in the sidebands, which were of the same mass width as the signal window, was used as the background contribution under the resonance peak. The nonlinearity of the background distribution was corrected based on the overall MC spectra of ϕp and nonresonant $\bar{K}\bar{K}p$ productions. This correction was significant in the K^+K^- mode, while it was negligible in the K^-p mode. Overestimation of background due to the $\Lambda(1520)$ tails in the sidebands was also corrected by using $\Lambda(1520)$ MC events.

Since many possible background processes other than the K^+K^-p final state were involved in the K^+p detection mode, two-step sideband subtractions were adopted for the background estimation instead of performing MC simulations. First, the K^+ missing mass spectrum was constructed for the sample which was selected within the K^- mass window of K^+p missing mass ($\pm 25 \text{ MeV}/c^2$). In order to ensure only the contribution from the K^+K^-p final state, this spectrum was corrected by subtracting the K^+ missing mass spectrum for the sample within the sideband regions of the K^- mass window. Further sideband subtraction was performed in the corrected K^+ missing mass spectrum by setting the $\Lambda(1520)$ signal window to 1.49–1.55 GeV/c^2 , as shown in Fig. 1(b). The linearity of the background spectra was reasonable in these sideband subtractions because only 5% variation was observed in the results with a change of the signal window widths.

Differential cross sections were measured in 30° bins in $K^{+/0}$ polar angle ($\theta_{K^{+/0}}$) in the c.m. system of photon and target nucleon. Acceptance factors were estimated in MC simulation taking into account the measured decay asymmetry of $\Lambda(1520)$. We confirmed that the ratio of luminosities estimated for the hydrogen and deuterium runs was consistent

with that of $\Lambda(1520)$ signal counts in the two data sets with detection of all three tracks in the K^+K^-p final state, which only arose from the interaction with protons. Figure 2(a) shows differential cross sections from protons at $1.9 < E_\gamma < 2.4 \text{ GeV}$ in all the detection modes. Cross sections at forward K^+ angles are more than 3 times larger than those at backward angles. This tendency does not contradict the existing theoretical pictures [3, 4, 5, 8] as Figure 2(a) shows a comparison with the prediction from a model, which considers the dominance of a contact-term contribution but no contribution from the K^* exchange under a rescaling by a cutoff mass of 650 MeV [5, 14]. In the region of $0^\circ < \theta_{K^+} < 30^\circ$, we have not resolved the discrepancy of results obtained in the two detection modes, but this may be caused by an interference with different background compositions. In Fig. 2(b), the differential cross sections measured at $19^\circ < \theta_{K^+} < 43^\circ$ are compared with the LAMP2 result. Theoretical calculations predict $\sim 1 \mu\text{b}$ or more at $E_\gamma \sim 2 \text{ GeV}$ with inputs from the LAMP2 result [3, 4, 5, 8], and the present results are smaller than those predictions. This measurement shall provide new information for theoretical models.

In the K^-p detection mode, the differential cross sections from protons and deuterons were compared as shown in Fig. 3. Here only the estimations using sideband subtractions are shown, and their deviations from MC-based results are typically 7%. By combining the cross sections measured in the range of $1.75 < E_\gamma < 2.4 \text{ GeV}$ and $120^\circ < \theta_{K^{+/0}} < 180^\circ$, the ratio of production of deuterons to that from protons was measured to be 1.02 ± 0.11 in the sideband-subtraction method. The $\Lambda(1520)$ photoproduction from neutrons was found to be strongly suppressed at backward K^0 angles. The observation of a large asymmetry between the productions from protons and neutrons conflicts with the model considering a dominance of t-channel K^* exchange [3], but can be explained by the model where the contact term plays a major

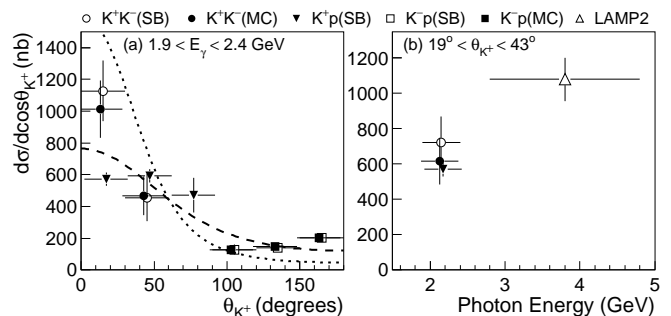


FIG. 2: (a) Differential cross sections from protons at $1.9 < E_\gamma < 2.4 \text{ GeV}$. The data points at forward K^+ angles come from the K^+K^- and K^+p detection modes, while those at backward angles are from the K^-p mode. The measurements using sideband-subtractions (SB) and Monte Carlo (MC) simulations are simultaneously plotted. The dashed line (dotted line) indicates a theoretical prediction for $E_\gamma = 1.85$ (2.35) GeV with K exchange and a contact term [14]. (b) Differential cross sections from this work and LAMP2 at $19^\circ < \theta_{K^+} < 43^\circ$.

role [5]. Larger cross sections were observed at lower energies as shown in Fig. 3, and this behavior is qualitatively consistent with a theoretical calculation in Ref. [5]. In the backward K^+ production from protons, cross sections also show an increase toward $\theta_{K^+}=180^\circ$ as shown in Fig. 2(a). This may indicate an additional contribution from u-channel diagrams, which are conventionally considered to be small in the theoretical models [3, 4, 5, 8].

The decay asymmetry of $\Lambda(1520)\rightarrow K^-p$ was studied in the production from protons by examining the distribution of K^- polar angle (θ_{K^-}) in the t-channel helicity frame (Gottfried-Jackson frame) [15]. In the case of K^* exchange, where the spin projection of helicity state is mostly of $S_z=\pm 3/2$, the K^- angular distribution is characterized by $\sin^2\theta_{K^-}$, while K exchange, composed of only $S_z=\pm 1/2$, results in an angular distribution of $\frac{1}{3} + \cos^2\theta_{K^-}$. At the same time, a contact-term contribution, whose dominance is favored by the cross section measurements, is shown to possess a large component of $S_z=\pm 3/2$ [5], and the relative strength of the contact term to the K exchange is determined by the $KN\Lambda(1520)$ coupling constant under gauge invariance [5, 6]. Figure 4(a) shows the K^- angular distribution using the sideband-subtraction methods in the K^+p and K^+K^- detection modes, which cover forward K^+ angles. Although an experimental acceptance in the K^+K^- mode is limited to the forward K^- direction, the K^- angular distribution in this mode is consistent with that in the K^+p mode. The obviously asymmetric distribution suggests a large interference, which is stronger than the results in LAMP2 [2] and CLAS [9]. We performed a fit to the K^- angular distribution measured in the K^+p mode by using a function $N(\alpha \sin^2\theta_{K^-} + (1-\alpha)(\frac{1}{3} + \cos^2\theta_{K^-}) + \beta \cos\theta_{K^-})$ [9], where the last term represents an interference with spin-1/2 background hyperons. The fraction of $S_z=\pm 3/2$ component (α) was measured to be 0.520 ± 0.063 in the photon energy range of 1.9–2.4 GeV, and clearly differed from the measurement by LAMP2 at higher energies, where the corresponding fraction was evaluated to be 0.880 ± 0.076 by a fit to Fig. 3 of Ref. [2]. The present result was closer to the value from the low-energy electroproduction by CLAS [9], which

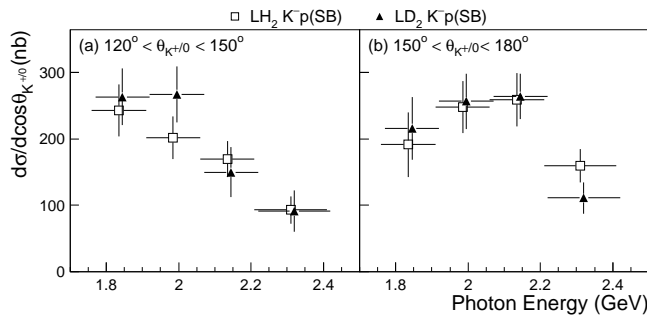


FIG. 3: Differential cross sections at backward K^{+0} angles in the K^-p detection mode. Results from the hydrogen and deuterium runs are simultaneously plotted as a function of photon energy for (a) $120^\circ < \theta_{K^{+0}} < 150^\circ$ and (b) $150^\circ < \theta_{K^{+0}} < 180^\circ$.

obtained 0.446 ± 0.038 for the virtual photon invariant mass of $0.9 < Q^2 < 1.2 \text{ GeV}^2$. One possible way to accommodate the observed ratio of the two spin projections under the dominance of a contact-term contribution is to introduce a small contribution from the K^* exchange with a destructive interference between $S_z=\pm 3/2$ components, as shown in Fig. 13 of Ref. [5]. The $K^*\Lambda(1520)$ coupling constant, which controls the strength of such an interference, is experimentally undetermined, and the theoretical predictions of its absolute value vary in the range of 0–15 [16]. The same fitting procedure was also performed for the K^- angular distribution at backward K^+ angles in the K^-p detection mode. Figure 4(b) shows the result with the sideband subtraction. While the interference was found to be weak, the fraction of $S_z=\pm 3/2$ was measured to be 0.631 ± 0.106 (0.545 ± 0.076) in the sideband-subtraction (MC-based) method for the photon energy range of 1.75–2.4 GeV. These fractions were similar to the result in the forward K^+ direction.

The photon beam asymmetry was also measured in the production from protons with K^+p detection for the K^+ angles less than 60° . $\Lambda(1520)$ signals produced from vertically and horizontally polarized photons were separately counted (N_V and N_H , respectively) as a function of K^+ azimuthal angle (ϕ). The beam asymmetry (Σ) was measured by the fit based on an equation $\Sigma P_\gamma \cos 2\phi = (kN_V - N_H)/(kN_V + N_H)$ [10], where P_γ was the polarization of the photon beam and k was a normalization factor of the two polarization samples. We determined Σ to be -0.01 ± 0.07 , which suggests zero within uncertainties. This value is consistent with the prediction of the theoretical model where the contact-term contribution is dominant [17], and thus the contribution from the t-channel K^* exchange is suggested to be small.

In summary, we studied $\Lambda(1520)$ photoproduction with liquid hydrogen and deuterium targets at $E_\gamma=1.75\text{--}2.4 \text{ GeV}$. At backward K^{+0} angles, we compared the cross sections from protons and deuterons. A strong suppression of the production from neutrons was observed as suggested in the theory advocating the importance of the contact term. By the decay asymmetry in the production from protons, the contri-

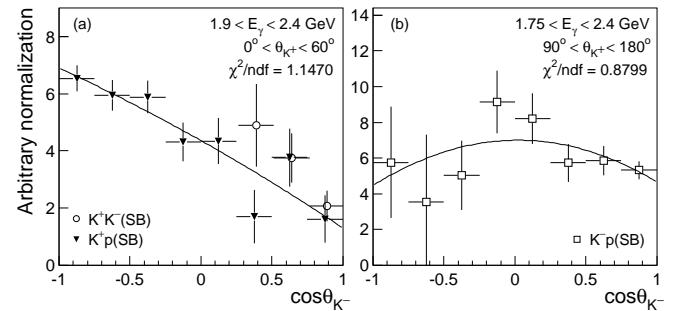


FIG. 4: K^- polar angle distributions in the t-channel helicity frame of $\Lambda(1520)$, produced from protons. Panels (a) and (b) show the results at forward and backward K^+ angles, respectively. The solid lines indicate fits by a linear combination of two spin-projection terms and an interference term.

bution from the $S_z = \pm 3/2$ component was determined to be nearly 50%. This fact may be explained by postulating a destructive interference between the $S_z = \pm 3/2$ components. The forward enhancement of the differential cross section and the small value of the photon beam asymmetry are also compatible with the interpretation adopting the contact term. Future precise measurements of the decay asymmetry and the photon beam asymmetry shall provide more accurate constraints on the value of $K^*N\Lambda(1520)$ coupling constant as well as details of reaction dynamics. Further theoretical studies will also be desired at a more quantitative level to explain the two asymmetry measurements.

This work is closely related to the possible production of Θ^+ . First, the LEPS experiment has reported the possibility of coherent photoproduction of $\gamma d \rightarrow \Lambda(1520)\Theta^+$ [11], where forward $\Lambda(1520)$ production plays an important role to induce the reaction of $K^+n \rightarrow \Theta^+$. The present measurement of elementary cross sections is essential to advance theoretical calculations of this reaction. Secondly, a comparison of the results in the LEPS [18] and CLAS [19] experiments might hint that Θ^+ photoproduction from protons is suppressed relative to that from neutrons. Such a target-isospin asymmetry may originate from the contact term [6] as suggested by the forward $\Lambda(1520)$ photoproduction in the present work.

The authors thank A. Hosaka and S.-i. Nam for theoretical discussions. We gratefully acknowledge the support of the staff at SPring-8 for providing excellent experimental conditions. This research was supported in part by the Ministry of Education, Science, Sports and Culture of Japan, the National Science Council of Republic of China (Taiwan), and the KOSEF of Republic of Korea.

-
- [2] D. P. Barber *et al.* (LAMP2 Collaboration), *Z. Phys. C* **7**, 17 (1980).
 - [3] A. I. Titov, B. Kämpfer, S. Daté, and Y. Ohashi, *Phys. Rev. C* **74**, 055206 (2006); A. I. Titov, B. Kämpfer, S. Daté, and Y. Ohashi, *Phys. Rev. C* **72**, 035206 (2005).
 - [4] A. Sibirtsev, J. Haidenbauer, S. Krewald, U.-G. Meißner, and A.W. Thomas, *Eur. Phys. J. A* **31**, 221 (2007).
 - [5] S.-I. Nam, A. Hosaka, and H.-C. Kim, *Phys. Rev. D* **71**, 114012 (2005).
 - [6] S.-I. Nam, A. Hosaka, and H.-C. Kim, *Phys. Lett. B* **633**, 483 (2006); S.-I. Nam, A. Hosaka, and H.-C. Kim, *J. Korean Phys. Soc.* **49**, 1928 (2006); S.I. Nam, A. Hosaka, and H.-C. Kim, *Phys. Lett. B* **579**, 43 (2004).
 - [7] M. Karlner and H. J. Lipkin, arXiv:hep-ph/0506084.
 - [8] H. Toki, C. García-Recio, and J. Nieves, *Phys. Rev. D* **77**, 034001 (2008).
 - [9] S. P. Barrow *et al.* (CLAS Collaboration), *Phys. Rev. C* **64**, 044601 (2001).
 - [10] M. Sumihama *et al.* (LEPS Collaboration), *Phys. Rev. C* **73**, 035214 (2006).
 - [11] N. Muramatsu (LEPS Collaboration), *Prog. Theor. Phys. Suppl.* **168**, 10 (2007).
 - [12] CERN Program Library Long Writeup W5013, 1993.
 - [13] J.M. Blatt and V.F. Weisskopf, *Theoretical Nuclear Physics* (John Wiley & Sons, New York, 1952).
 - [14] S.-I. Nam and A. Hosaka (private communication).
 - [15] K. Schilling, P. Seyboth, and G. Wolf, *Nucl. Phys.* **B15**, 397 (1970).
 - [16] T. Hyodo, S. Sarkar, A. Hosaka, and E. Oset, *Phys. Rev. C* **73**, 035209 (2006).
 - [17] S.-i. Nam, K.-S. Choi, A. Hosaka, and H.-C. Kim, *Phys. Rev. D* **75**, 014027 (2007).
 - [18] T. Nakano *et al.* (LEPS Collaboration), *Phys. Rev. Lett.* **91**, 012002 (2003); T. Nakano *et al.* (LEPS Collaboration), *Phys. Rev. C* **79**, 025210 (2009).
 - [19] M. Battaglieri *et al.* (CLAS Collaboration), *Phys. Rev. Lett.* **96**, 042001 (2006); R. De Vita *et al.* (CLAS Collaboration), *Phys. Rev. D* **74**, 032001 (2006).

[1] W.-M. Yao *et al.* (Particle Data Group), *J. Phys. G* **33**, 1 (2006).